NONRESONANT THIRD ORDER HYPERPOLARIZABILITY OF RARE GASES AND N_2 DETERMINED BY THIRD HARMONIC GENERATION

H.J. LEHMEIER, W. LEUPACHER and A. PENZKOFER

Naturwissenschaftliche Fakultät II – Physik, Universität Regensburg, 8400 Regensburg, Fed. Rep. Germany

Received 26 June 1985; revised manuscript received 23 August 1985

The third order hyperpolarizability $\gamma^{(3)}_{1111}(-\omega_3;\omega_1,\omega_1,\omega_1)$ of the rare gases He, Ne, Ar, Kr, Xe and of N_2 are determined by third harmonic generation involving picosecond light pulses of a Nd-glass laser. The results are compared with reported experimental and theoretical values.

1. Introduction

Experimental determinations of nonresonant third order hyperpolarizabilities of gases are scarce [1–4]. Their measurement by third harmonic generation or collinear four-photon frequency mixing [1–3] is complicated by the fact that these processes occur in all media along the path of the laser beams and that tight focusing of laser light into a normal dispersive sample results in no third harmonic or frequency mixing output at all [2,3,5,6].

In this paper we determine third order hyperpolarizabilities of the rare gases He, Ne, Ar, Xe, Kr and of the molecular gas N_2 by third harmonic generation. The problem of third harmonic generation along the light path outside the sample is avoided by putting the gas cells into a vacuum chamber behind the focal region of the slightly focused laser beam and using cell windows of thickness equal to an even integer of the coherence length $\pi/\Delta k$ of the interaction [4,7] (Maker fringe minima [8]).

Single picosecond light pulses of a passively mode-locked Nd-glass laser are used in the experiments. The obtained third order hyperpolarizabilities are compared with previous measurements with a ruby laser [1,3] and with reported theoretical values obtained by several approximative quantum mechanical approaches [3,9–16].

2. Theory

The nonlinear polarization responsible for third harmonic generation $\omega_1 + \omega_1 + \omega_1 \rightarrow \omega_3$ is given by

$$P_{\mathrm{NL}} = 4\epsilon_0 \chi^{(3)} : EEE, \tag{1}$$

SI units in the notation of ref. [17] are used. In the collinear plane-wave approximation of linearly polarized light, i.e. $E = E_1 + E_3$ with $E_j = (E_j, 0, 0)$ and $P_{\mathrm{NL},j} = (P_{\mathrm{NL},j}, 0, 0)$ $(j = 1, 3)$ where $E_j = \{E_{j0} \times \exp[\mathrm{i}(k_j z - \omega_j t)] + \mathrm{c.c.}\}/2$ and $P_{\mathrm{NL},j} = \{P_{\mathrm{NL},j0} \times \exp[\mathrm{i}(k_j z - \omega_j t)] + \mathrm{c.c.}\}/2$, the nonlinear polarization responsible for third harmonic generation is given by

$$P_{\mathrm{NL},30} = \epsilon_0 \chi^{(3)}_{1111}(-\omega_3;\omega_1,\omega_1,\omega_1) E^3_{10} \exp(-\mathrm{i}\Delta k z), \tag{2}$$

$\Delta k = k_3 - 3k_1 = (n_3\omega_3 - 3n_1\omega_1)/c = 3\omega_1(n_3 - n_1)/c$ is the wave vector mismatch. c is the vacuum light velocity. $\chi^{(3)}_{1111}(-\omega_3;\omega_1,\omega_1,\omega_1)$ is abbreviated by $\chi^{(3)}$ in the following.

In nonabsorbing media the plane wave equation reduces to

$$(\partial/\partial z) E_{30} = (\mathrm{i}\omega_3/2n_3c)\chi^{(3)} E^3_{10}(z) \exp(-\mathrm{i}\Delta k z). \tag{3}$$

Neglecting pump pulse depletion $[E_{10}(z) = E_{10}]$ the plane wave solution is

$$E_{30}(l) = (\mathrm{i}\omega_3/2n_3c)\chi^{(3)} E^3_{10}[\sin(\Delta k l/2)]/(\Delta k/2). \tag{4}$$

0 030-4018/85/$03.30 © Elsevier Science Publishers B.V. (North-Holland Physics Publishing Division)

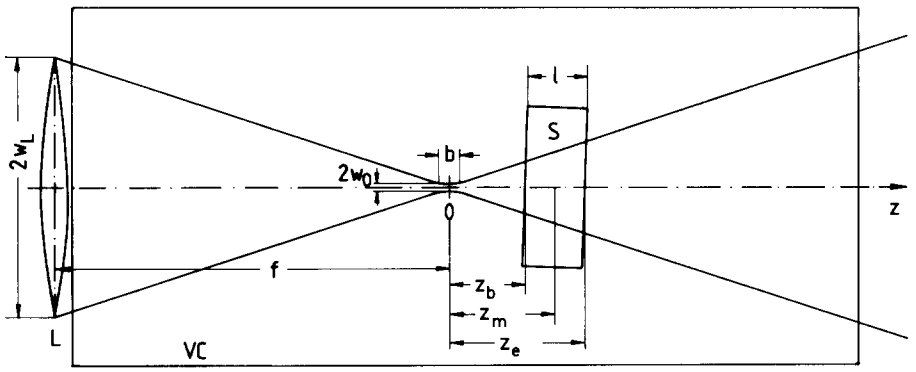

Fig. 1. Schematic of light path through vacuum chamber and gas sample. L, lens (f = 30.5 cm); VC, vacuum chamber; S, sample (length l, center position z_m); b, confocal parameter [$w(b/2) = 2^{1/2}w_0$]; $2w_0$, smallest spot size (at z = 0; full 1/e width of electric field strength); $2w_L$, spot size at entrance to lens.

The third harmonic intensity is obtained by use of the relation $I_j = (n_j c\epsilon_0/2)|E_{j0}|^2$ and eq. (4):

$$I_3 = \frac{\omega_3^2}{n_3 n_1^3 c^4 \epsilon_0^2} |\chi^{(3)}|^2 I_1^3 \frac{\sin^2(\Delta k l/2)}{(\Delta k/2)^2}. \tag{5}$$

In the experiments the energy conversion $\eta = W_3/W_1$ is measured with $W_j = \int_0^\infty 2\pi r dr \int_{-\infty}^{\infty} I_j(r,t)dt$ (j = 1, 3). For gaussian pump pulses the input intensity is $I_1(r,t) = I_{10}\exp(-r^2/r_0^2)\exp(-t^2/t_0^2)$ and the third harmonic energy conversion is derived from eq. (5) to be

$$\eta = \frac{W_3}{W_1} = \frac{1}{3^{3/2}} \frac{\omega_3^2}{n_3 n_1^3 c^4 \epsilon_0^2} |\chi^{(3)}|^2 I_{10}^2 \frac{\sin^2(\Delta k l/2)}{(\Delta k/2)^2}. \tag{6}$$

In the gas investigations sample cells of some centimeter length have to be used to obtain enough signal and the beam divergence in the sample has to be considered. Our experimental situation is sketched in fig. 1. Lens L (focal length f) focuses the light into the vacuum chamber VC. The sample cell S of thickness l is centered at distance z_m behind the focus z = 0. The spatial and temporal field strength of the input pulse in the vacuum chamber at position z is given by [3,5, 6,18,19]

$$E_{10}(r,z,t) = \frac{E_{10}(0)}{1 + i2z/b} \exp\left(\frac{k_1 r^2}{b(1 + i2z/b)}\right) \times \exp(-t^2/2t_0^2). \tag{7}$$

The intensity distribution is

$$I_1(r,z,t) = \frac{I_{10}(0)}{1 + (2z/b)^2} \times \exp\left(-\frac{r^2}{r_0^2(0)[1 + (2z/b)^2]} - \frac{t^2}{t_0^2}\right), \tag{8}$$

$b = k_1 w_0^2 = 2\pi n_1 w_0^2/\lambda_1$ is the confocal parameter. w_0 is the beam waist (1/e-field radius) at the focal point z = 0. It is determined by the beam waist w_L at lens L, the laser wavelength λ_1 and the focal length f according to $w_0 = 2f/k_1 w_L = f\lambda_1/\pi n_1 w_L$ [20]. The beam waist at position z is $w(z) = w_0[1 + (2z/b)^2]^{1/2}$ while the beam radius r_0 (1/e intensity radius) at z = 0 is $r_0(0) = 2^{-1/2}w_0$ and the beam radius at z is $r_0(z) = 2^{-1/2}w(z)$.

The differential equation for third harmonic generation by gaussian beams is [19]

$$\left(\frac{\partial}{\partial r^2} + \frac{1}{r}\frac{\partial}{\partial r} + 2ik_3 \frac{\partial}{\partial z}\right) E_{30} = -\frac{\omega_3^2}{c^2}\chi^{(3)} \frac{E_{10}^3(0)}{(1 + i2z/b)^3} \times \exp\left(-\frac{3k_1 r^2}{b(1 + i2z/b)} - \frac{3t^2}{2t_0^2} - i\Delta k z\right). \tag{9}$$

Its solution is [5,18,19] (for z_b and z_e see fig. 1):

$$E_{3b}(z_e) = i\frac{\omega_3}{2n_3c}\chi^{(3)}\frac{E_{10}^3(0)}{1+i2z_e/b} \times \exp\left(-\frac{3r^2}{w_0^2(1+i2z_e/b)} - \frac{3t^2}{2t_0^2} - i\Delta k z_b\right) \times \int_{z_b}^{z_e} \frac{\exp(-i\Delta k z')}{(1+i2z'/b)^2}\,dz'. \quad (10)$$

From this expression the third harmonic intensity is found to be

$$I_3(z_e) = \frac{\omega_3^2|\chi^{(3)}|^2 I_{10}^3(0)}{n_3 n_1^3 c^4 \epsilon_0^2 [1+(2z_e/b)^2]} \times \exp\left(-\frac{3r^2}{r_0^2(0)[1+(2z_e/b)^2]} - \frac{3t^2}{t_0}\right) \times \left|\int_0^l \frac{\exp(-i\Delta k z)}{[1+i2(z_b+z)/b]^2}\,dz\right|^2. \quad (11)$$

Finally the energy conversion is given by

$$\eta = \frac{W_3}{W_1} = \frac{\omega_3^2|\chi^{(3)}|^2}{3^{3/2}n_3 n_1^3 c^4 \epsilon_0^2} I_{10}^2(z_m) \times \left|\int_0^l \frac{1+(2z_m/b)^2}{[1+i2(z_b+z)/b]^2}\exp(-i\Delta k z)dz\right|^2, \quad (12)$$

where $I_{10}(z_m) = I_{10}(0)/[1+(2z_m/b)^2]$ is the fundamental peak pulse intensity at the center position z_m of the sample. For $b \gg l$, eq. (12) becomes identical to eq. (6).

The energy conversion η is the ratio of third harmonic energy at the end of the sample inside the cell window to the input fundamental pulse energy at the beginning of the sample inside the cell window. The reflection losses of the windows are taken care of in the experiments [4,7].

The nonlinear susceptibility $\chi^{(3)}$ of the gases may be expressed in terms of the nonlinear hyperpolarizability $\gamma^{(3)}$ by [7]

$$\chi_{1111}^{(3)}(-\omega_3;\omega_1,\omega_1,\omega_1) = \epsilon_0^{-1}NL^{(4)}\gamma_{1111}^{(3)}(-\omega_3;\omega_1,\omega_1,\omega_1) = (N_0 p T_0 L^{(4)}/\epsilon_0 p_0 T)\gamma_{1111}^{(3)}(-\omega_3;\omega_1,\omega_1,\omega_1), \quad (13)$$

$L^{(4)} \approx (n_1^2+2)^3(n_3^2+2)/81$ is the Lorentz-local-field correction factor. The number density N at pressure p and temperature T is related to the number density $N_0 = p_0/kT_0 = 2.6869 \times 10^{19}$ cm^{-3} at standard pressure $p_0 = 1$ atm $= 1.0133 \times 10^5$ Pa and standard temperature $T_0 = 273.15$ K by $N = N_0 p T_0/p_0 T$.

The linear refractive index n is related to the linear polarizability $\chi^{(1)}(-\omega;\omega)$ by $n^2 - 1 = \chi^{(1)} = NL^{(1)}\gamma^{(1)}/\epsilon_0$ with $L^{(1)} = (n^2+2)/3$. The temperature and pressure dependence of n is given by

$$\frac{n^2-1}{n^2+2} = \frac{n_0^2-1}{n_0^2+2}\frac{pT_0}{p_0 T}, \quad (14)$$

n_0 is the refractive index at standard conditions ($p_0 = 1$ atm, $T_0 = 273.15$ K). Its value is determined by dispersion formulas [21,22]. The refractive index n at pressure p and temperature T is derived from eq. (14) to be

$$n = \left(2\frac{n_0^2-1}{n_0^2+2}\frac{pT_0}{p_0 T} + 1\right)^{1/2}\left(1 - \frac{n_0^2-1}{n_0^2+2}\frac{pT_0}{p_0 T}\right)^{-1/2}. \quad (15)$$

Eqs. (12), (13) and (15) are applied to determine the third order hyperpolarizabilities $\gamma^{(3)}$ of the investigated gases.

3. Experiment

The experimental arrangement is the same as used in ref. [4]. Two gas cells of length $l = 4.52$ cm (He, Ne) and $l = 1.18$ cm (all other gases) were constructed. The gas handling system allowed evacuating, flushing and filling. High purity rare gases and nitrogen gas were used. The gas pressure was varied between 0 and 0.9×10^5 Pa (0.9 bar) for the short cell and between 0.9×10^5 and 2.5×10^5 Pa for the long cell. Thin windows (thickness around 0.2 mm) of fused silica

were selected to achieve zero third harmonic contribution at the entrance and exit (Maker fringe minima) under a small tilting angle of the cell. Single picosecond laser pulses from a passively mode-locked Nd-phosphate glass laser have been applied (wavelength $\lambda_1 = 1.055$ μm, duration $\Delta t \approx 5$ ps, peak intensity in sample $I_{10}(z_m) \approx 2 \times 10^9$ W/cm^2). The input pulse energy and peak pulse intensity [23] together with the third harmonic pulse energy are measured for each laser shot. The energy detectors (fast vacuum photocell at ω_1 and photomultiplier at ω_3) are calibrated relative to one another with a pyroelectric energy meter. The input pulse has a beam radius $r_{0,L} = w_L/\sqrt{2} = 5.6$ mm in front of lens L (fig. 1) resulting in a confocal parameter of $b = 0.44$ cm ($f = 30.5$ cm). The sample cells are centered $z_m = 8$ cm behind the focal position.

4. Results

The normalized energy conversions $\eta/I_{10}^2(z_m)$ versus pressure p are presented in fig. 2 for N_2, Ar, Kr, and Xe and in fig. 3 for He and Ne. The solid curves indicate the best fit. They are calculated by use of eq. (12) (gaussian focused beam) while the dashed curves belong the eq. (6) (non-focused beam) with the same parameters as used for the solid curves. The non-fo-

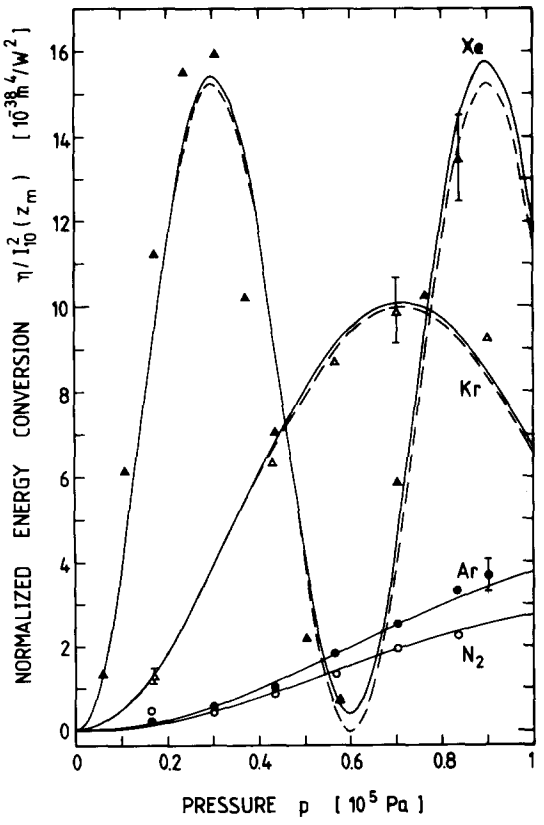

Fig. 2. Third harmonic light generation in N_2, Ar, Kr, Xe. Normalized energy conversion $\eta/I_{10}^2(z_m)$ versus pressure is shown. Solid curves present best fit of eq. (12) to experimental points. N_2: (○), $\gamma^{(3)} = 2.38 \times 10^{-63}$ Cm^4/V^3; Ar: (●), $\gamma^{(3)} = 2.65 \times 10^{-63}$ Cm^4/V^3; Kr: (△), $\gamma^{(3)} = 7.22 \times 10^{-63}$ Cm^4/V^3; Xe: (▲), $\gamma^{(3)} = 2.12 \times 10^{-62}$ Cm^4/V^3. Dashed curves are calculated by use of eq. (6) with same parameters. Temperature $T = 296$ K. Wavelength $\lambda_1 = 1.055$ μm.

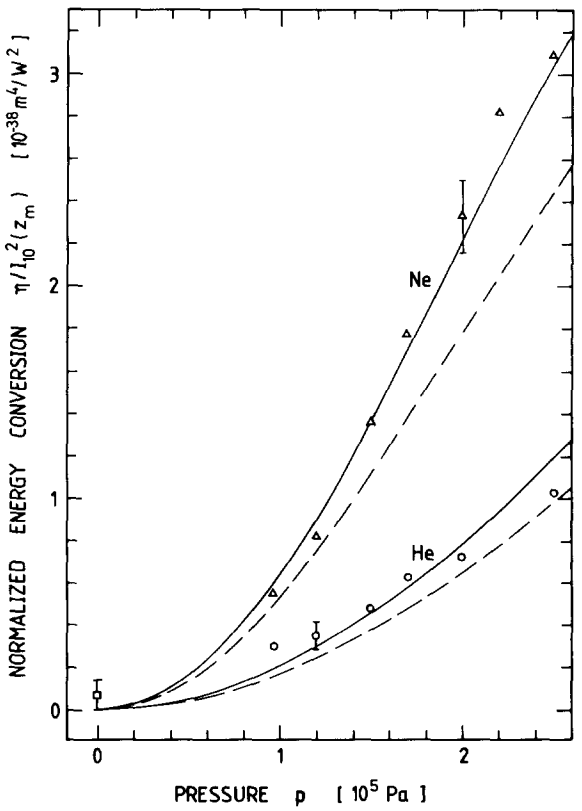

Fig. 3. Third harmonic generation in He and Ne. Solid curves give best fit of eq. (12) to experimental points (gaussian focused beam) with $\gamma^{(3)} = 1.13 \times 10^{-64}$ Cm^4/V^3 (He, ○) and $\gamma^{(3)} = 2.03 \times 10^{-64}$ Cm^4/V^3 (Ne, △). Dashed curves are calculated by use of eq. (6) (unfocused beams) with same parameters. Temperature $T = 296$ K. Wavelength $\lambda_1 = 1.055$ μm.

Table 1
Parameters of investigated gases. Subscript 0 indicates standard pressure and temperature condition (p_0 = 1 atm, T_0 = 0°C). $\lambda_1 = 2\pi c/\omega_1$ = 1.055 μm

Gas	$(n_{10}-1)\times 10^5$	$(n_{30}-1)\times 10^5$	Δk_0 [cm^{-1}]	$l_{coh,0}$ [cm]	$\chi_0^{(3)}/\chi_0^{(3)}(He)$ c)	$\xi/f^2/\xi/f^2(He)$ d)	$\gamma^{(3)}_{1111}(-\omega_3,\omega_1,\omega_1,\omega_1)$ [10^{-64} Cm^4/V^3]	[10^{-39} esu]
He	3.472 a)	3.532 c)	0.1067	29.437	1	1	1.13	0.914
Ne	6.678 a)	6.791 a)	0.2021	15.545	1.8	0.13	2.03	1.64
Ar	27.863 a)	28.977 a)	1.990	1.579	23.5	5.5×10^{-3}	26.5	21.4
Kr	42.222 a)	44.514 a)	4.095	0.767	64.0	3.4×10^{-3}	72.2	58.4
Xe	68.389 a)	73.848 a)	9.752	0.322	188.2	1.2×10^{-3}	212	172
N_2	29.607 b)	31.017 b)	2.519	1.247	21.1	3.9×10^{-3}	23.8	19.3

a) Ref. [21]. b) Ref. [22]. c) $\chi_0^{(3)}(He) = 3.43\times10^{-28}$ m^2/V^2. d) $\xi/f^2(He) = 1.17\times10^{54}$ m^{-2} s^{-2}.

cused interaction with equal intensity $I_{01}(z_m)$ results in lower energy conversion. In case of the short sample cell (fig. 2) eq. (12) and eq. (6) lead to nearly the same result. The standard refractive indices used in the calculations together with the obtained third order nonlinear susceptibility at standard conditions and the nonlinear hyperpolarizability are listed in table 1. The relative error of the normalized energy conversion is estimated to be about ±0.2 leading to a relative error of the third hyperpolarizabilities of ±0.1.

According to the anharmonic oscillator model the third order hyperpolarizability is related to the linear polarizability by [4,7]

$$\gamma^{(3)}(-\omega_3;\omega_1,\omega_1,\omega_1) = \xi(m/4f^2e^4)\gamma_1^{(1)3}\gamma_3^{(1)}, \quad (16)$$

where ξ is the anharmonic coupling constant, m the electron mass, f the oscillator strength and e the electron charge. The expression of eq. (16) may be rewritten with the add of eq. (13) to (Miller's rule [24]):

$$\chi^{(3)}_{1111,0}(-\omega_3;\omega_1,\omega_1,\omega_1) = (\xi/f^2)(\epsilon_0^3 m/4N_0^3e^4)(n_{10}^2-1)^3(n_{30}^2-1). \quad (17)$$

In table 1 the effective anharmonic coupling constant ξ/f^2 is listed. The values decrease with rising molecules mass of the gases. Helium shows the strongest anharmonic coupling.

In table 2 the measured $\gamma^{(3)}$-values are compared with previously reported experimental and theoretical

Table 2
Comparison of third-order hyperpolarizabilities. Fundamental wavelength λ_1 = 694.3 nm ($\gamma^{(3)}$[esu] = $8.0888\times10^{24}\gamma^{(3)}$ [SI] [17]). (a)–(c) experimental results, (d)–(i) theoretical results.

Gas	$\tilde{\nu}_0$ [cm^{-1}]	$\gamma^{(3)}_{1111}(-\omega_3,\omega_1,\omega_1,\omega_1)$ [10^{-39} esu]									$\gamma^{(3)}_{1111}(-\omega;\omega,0,0)$
		(a)	(b)	(c)	(d)	(e)	(f)	(g)	(h)	(i)	[10^{-39} esu]
He	197 316	1.00	0.6–5.3	1.00	1	1.16	0.85	0.225	3.25	1.08	1.13
Ne	208 087	1.79	1–13.2	2.23	–	2.55		0.425	3.1	2.6	2.13
Ar	137 568	24.8	15.5–192	31.5	–	–		7	21.3	48.4	24.6
Kr	119 190	69.8	45.4–605	96.5	–	–		17.8	97.8	–	58.3
Xe	99 946	217	81.6–734	245	–	–		55.4	–	–	163
N_2	137 916	22.3	8.9–80	26.8	–	–		–	–	–	–

(a) This work. Wavelength dependence of eq. (18) applied to data of table 1.
(b) Refs. [1] and [3]. Values quoted here rae a factor 4 smaller than those in refs. [1] and [3] because of our definition of $\gamma^{(3)}$.
(c) Refs. [1] and [3]. Values are normalized to helium with $\gamma^{(3)}_{1111}(He) = 1\times10^{-39}$ esu.
(d) Ref. [12]. (e) Ref. [16]. (f) Ref. [15]. (g) Ref. [11]. (h) Ref. [14]. (i) Ref. [10].

results. Since the previous third harmonic generation work [1,3] belongs to the ruby laser wavelength λ_1 = 694.3 nm, our results are transferred to this wavelength using the relation

$$\gamma^{(3)}(-\omega_{3a};\omega_{1a},\omega_{1a},\omega_{1a}) \approx \frac{\omega_0-\omega_{3b}}{\omega_0-\omega_{3a}}\gamma^{(3)}(-\omega_{3b};\omega_{1b},\omega_{1b},\omega_{1b},\omega_{1b}), \quad (18)$$

$\omega_0 = 2\pi c\tilde{\nu}_0$ is set equal to the lowest electronic transition frequency that enters the refractive index dispersion formula [22] (near first absorption peak). The $\tilde{\nu}_0$ values are listed in table 2. Eq. (18) is obtained by separating out the smallest frequency denominator of the perturbation expansion [7,12,15].

The experimental data of Ward and New [1,3] (column b of table 2) fit within the rather large error bars with our measurements. Their normalized values $\gamma^{(3)}/\gamma^{(3)}$(He) agree well with our results (column c). The theoretical hyperpolarizabilities of He obtained by Sitz and Yaris [12] (column d), Langhoff et al. [10] (column i), Mizuno [16] (column e), and Klingbeil et al. [15] (column f) agree rather well with our experimental value. For the other rare gases the theoretical hyperpolarizability values differ considerably from our measurements. The absolute values of Dawes [11] (column g, approximation of perturbation theory) are a factor of 4.5 too small but the ratios $\gamma^{(3)}/\gamma^{(3)}$(He) agree very well with our results. In the last column of table 2 the hyperpolarizabilities $\gamma^{(3)}_{1111}(-\omega;\omega,0,0)$ obtained by dc Kerr effect measurements [25] are listed ($\lambda = 2\pi c/\omega$ = 632.8 nm). They agree rather well with our third harmonic generation results indicating that in rare gases at low pressure no zero-frequency resonances contribute to the dc-Kerr hyperpolarizability.

5. Conclusions

The third-order hyperpolarizabilities $\gamma^{(3)}_{1111}(-\omega_3;\omega_1,\omega_1,\omega_1)$ of He, Ne, Ar, Kr, Xe and N_2 are measured at wavelength λ_1 = 1.055 μm with an experimental arrangement that avoids contributions to third harmonic generation outside the substance under investigation. The reported values are accurate enough to test the accuracy of theoretical $\gamma^{(3)}$ calculations.

The molecular gas N_2 behaves similar as the rare gas Ar with respect to linear spectroscopic data (refractive indices, lowest transition frequency) and the nonlinear hyperpolarizability.

References

[1] G.H.C. New and J.F. Ward, Phys. Rev. Letters 19 (1967) 556.
[2] W.G. Rado, Appl. Phys. Letters 11 (1967) 123.
[3] J.F. Ward and G.H.C. New, Phys. Rev. 185 (1969) 57.
[4] M. Thalhammer and A. Penzkofer, Appl. Phys. B32 (1983) 137.
[5] R. Fischer and L.W. Wieczorek, Ann. Phys. 7. Folge 35 (1978) 57.
[6] Y.M. Yiu, T.J. McIlrath and R. Mahon, Phys. Rev. A20 (1979) 2470.
[7] W. Leupacher and A. Penzkofer, Appl. Phys. B36 (1985) 25.
[8] P.D. Maker and R.W. Terhune, Phys. Rev. 137 (1965) A801.
[9] L.L. Boyle, A.D. Buckingham, R.L. Disch and D.A. Dummur, J. Chem. Phys. 45 (1966) 1318.
[10] P.W. Langhoff, J.D. Lyons and R.P. Hurst, Phys. Rev. 148 (1966) 18.
[11] E.L. Dawes, Phys. Rev. 169 (1968) 47.
[12] P. Sitz and R. Yaris, J. Chem. Phys. 49 (1965) 3546.
[13] M.N. Grasso, K.T. Chung and R.P. Hurst, Phys. Rev. 167 (1968) 1.
[14] B.P. Tripathi, R.K. Laloraya and S.L. Srivastava, Phys. Rev. A4 (1971) 2076.
[15] R. Klingbeil, V.G. Kaveeshwar and R.P. Hurst, Phys. Rev. A4 (1971) 1760.
[16] J. Mizuno, J. Phys. B: Atom. Molec. Phys. 5 (1972) 1875.
[17] R.W. Minck, R.W. Terhune and C.C. Wang, Appl. Optics 5 (1966) 1595.
[18] G.C. Bjorklund, IEEE J. Quant. Electron. QE-11 (1975) 287.
[19] J.F. Reintjes, Nonlinear optical parametric processes in liquids and gases (Academic Press, Orlando, 1984).
[20] A. Yariv, Quantum electronics (2nd Edition, Wiley, New York, 1975) ch. 6.
[21] A. Dalgarno and A.E. Kingston, Proc. Roy. Soc. A259 (1966) 424.
[22] Landolt-Börnstein, Teil 8, Optische Konstanten, eds. K.H. Hellwege and A.M. Hellwege (Springer, Berlin, 1962) p. 6-885.
[23] A. Penzkofer, D. vonder Linde and A. Laubereau, Optics Comm. 4 (1972) 377.
[24] R.C. Miller, Appl. Phys. Letters 5 (1964) 17.
[25] A.D. Buckingham and D.A. Dummur, Trans. Faraday Soc. 64 (1968) 1776.